JACS
JOURNAL OF THE AMERICAN CHEMICAL SOCIETY

COMMUNICATION

pubs.acs.org/JACS

Synthesis of NanoQ, a Copper-Based Contrast Agent for High-Resolution Magnetic Resonance Imaging Characterization of Human Thrombus

Dipanjan Pan,*[,†] Shelton D. Caruthers,[†] Angana Senpan,[†] Ceren Yalaz,[†] Allen J. Stacy,[†] Grace Hu,[†] Jon N. Marsh,[†] Patrick J. Gaffney,[‡] Samuel A. Wickline,[†] and Gregory M. Lanza[†]

[†]C-TRAIN and Division of Cardiology, Washington University School of Medicine, 4320 Forest Park Avenue, Saint Louis, Missouri 63108, United States

[‡]Department of Surgery, St. Thomas' Hospital, London SE1 7EH, U.K.

Supporting Information

ABSTRACT: A new site-targeted molecular imaging contrast agent based on a nanocolloidal suspension of lipid-encapsulated, organically soluble divalent copper has been developed. Concentrating a high payload of divalent copper ions per nanoparticle, this agent provides a high per-particle r1 relaxivity, allowing sensitive detection in T1-weighted magnetic resonance imaging when targeted to fibrin clots in vitro. The particle also exhibits a defined clearance and safety profile in vivo.

Atherosclerotic plaque rupture induces thrombus formation, which can progress immediately to myocardial infarction and stroke.[1,2] In many instances, however, plaque ruptures are small and transiently elicit local myocardial symptoms or embolize to induce transient ischemic attacks. Despite recent improvements in high-spatial-resolution carotid magnetic resonance imaging (MRI) techniques, the detection of subtle intimal ruptures and microthrombosis in atherosclerotic vessels is complicated and not routinely performed in the clinic. However, molecular MRI of microthrombosis using targeted contrast agents could offer sensitive detection and rapid diagnosis.[3]

To date, two types of MRI contrast agents have garnered the most clinical attention: those based on iron or gadolinium. Gadolinium molecular imaging agents certainly offer the best opportunity to achieve bright (T1-weighted), sensitive contrast enhancement shortly after intravenous administration, in contradistinction to most T2*-weighted agents, which require 24 h or more for background interference from persistently circulating iron particles to abate. Unfortunately, the discovery of nephrogenic systemic fibrosis has created safety questions for Gd-based agents, including the contraindication of use for individuals with significant renal dysfunction or after liver transplant.[4] These concerns have triggered reconsideration of alternative approaches based on non-lanthanide metals for T1-weighted imaging, such as manganese (Mn).[5]

Copper (Cu) is a non-lanthanide metal that has remained mostly unexplored as an MRI contrast agent. Copper is paramagnetic and has intrinsic properties favorable for MRI contrast enhancement, specifically an unpaired electron in its outermost orbital. Copper is a critical nutrient, serves as a cofactor for many biological processes, and generally is well-tolerated in humans.[6a] There have been only a few reports on induction of pathological changes in cultured human skeletal muscle cells through divalent copper intoxication, but the mechanism is unclear.[6b] To the best of our knowledge, only a single report describing the development of a "hard" copper-based nanoparticle is available.[7] In that work, Cu^{3+} ions in combination with gold (Au_3Cu) as nanoshells and nanocapsules were reported as a blood pool MRI contrast agent (the proton relaxivity was estimated in terms of molar relaxivity based on the number of nanoparticles per mM $\approx 3 \times 10^4$ mM^{-1} s^{-1} for nanocapsules.) Unfortunately, hard particles (>10 nm) are poorly eliminated in humans and often are very slowly or never biometabolized, which creates biosafety questions. Our objective was to develop and characterize a new "soft" nanoparticle-based contrast agent platform containing paramagnetic divalent copper with a high paramagnetic metal capacity for sensitive MRI detectability that is rapidly bioeliminated, preventing the bodily accumulation of copper, which can elicit unintended adverse effects.

Here we report for the first time the synthesis and MRI characterization of copper oleate nanocolloids (NanoQ) based on divalent copper (Cu^{2+}). We hypothesized that fibrin-targeted NanoQ nanoparticles could deliver millions of copper atoms specifically to thrombus and exhibit strong T1w MRI contrast enhancement of the target. Importantly, NanoQ was designed for vascular retention based on particle size (i.e., >200 nm) to avoid undesired extravasation and targeting of healed intraplaque hemorrhages or other nonvascular fibrin deposits. Moreover, the copper atoms are uniquely sequestered within the core matrix, which is nonintuitive for paramagnetic agents intended to influence the spins of water protons in the surrounding medium but important to avoid potential adverse blood contact with blood constituents, particularly complement, and eliminate possible interactions with homing ligands on the functionalized surface.

The surfactant mixture for the targeted nanoparticles was composed of phosphatidylcholine (lecithin-egg PC, 99 mol % lipid constituents) and biotin−caproyl−PE (1 mol %; PE = phosphatidylethanolamine). To achieve a loading of more than 2% (w/v), commercially available copper(II) oleate was

Received: March 2, 2011
Published: May 23, 2011

dx.doi.org/10.1021/ja201918u | J. Am. Chem. Soc. 2011, 133, 9168–9171

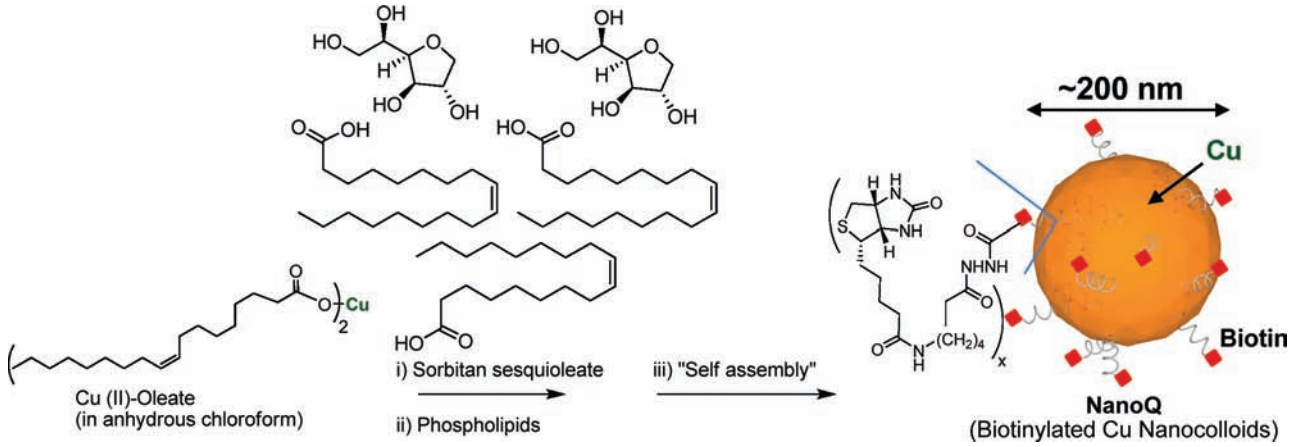

Figure 1. Synthesis of NanoQ: (i) suspension of copper(II) oleate (anhydrous chloroform solution) with sorbitan sesquioleate [>2% (w/v)] followed by vortexing, mixing, and evaporation of chloroform under reduced pressure at 45 °C; (ii) thin-film formation from a phospholipid mixture at 40 °C followed by drying under vacuum overnight at 45 °C; (iii) self-assembly by homogenization at 20 000 psi (137.9 MPa) for 4 min at 0 °C.

suspended with sorbitan sesquioleate to produce a homogeneous suspension of the inner matrix. Self-assembled NanoQ particles were formed by high-pressure homogenization (137 MPa, i.e., ~20 000 psi, for 4 min) at 4 °C in the presence of the aqueous dispersed surfactant mixture (Figure 1). The presence of the caproylbiotin moiety in the NanoQ presented nominally 18 000 biotin molecules per nanoparticle, which were used for avidin−biotin coupling of the homing ligand to the nanoparticles in a demonstration of concept. The concentration of copper in the nanoparticle was determined by ICP−OES as 67.2 mg/L of colloidal suspension of NanoQ, corresponding to ~14 000 copper atoms per particle. A nontargeted control nanoparticle was synthesized in a similar way that excluded the incorporation of biotin in the surfactant mixture. For synthesis and characterization details, see the Supporting Information (SI).

Multiple analytical techniques were employed to characterize these particles. Hydrodynamic particle sizes for the biotinylated NanoQ were 210 ± 6 nm a with narrow distribution [polydispersity index (PDI) = 0.17] (Figure S1a in the SI). The anhydrous-state properties were determined by atomic force microscopy (AFM) analyses after the aqueous suspension was drop-deposited on a glass slide. The particle height was calculated to be 78 ± 12 nm (Figure S1b). UV−vis spectroscopy confirmed the absorbances at 650−750 nm, corresponding to the presence of multiple Cu atoms in oleate complexes. The particle stability with time and over the physiological pH range 5.9−9.5 (Figures S2 and S3) and successful phospholipid encapsulation were confirmed through light scattering measurements and the presence of negative electrophoretic potential (ζ) values (i.e., −15 mV). These uniquely constructed nanocolloids possess long shelf-life stability and retain the particle integrity for viable clinical translation. In order to test the stability of the copper binding in the particle, a dissolution experiment was undertaken. In this study, total release of only <2% was observed over 3 days against an infinite sink. These results indicate a loading efficiency of 98−99% with excellent retention in dissolution and without significant in vitro immediate release of copper in the presence rabbit plasma, saline, or human plasma albumin at 37 °C. The release of the copper oleate was monitored by UV−vis spectroscopy over the 600−700 nm wavelength range (see Figure S1c and the stability data in the SI). The study further confirmed that copper is well-retained within the particle membrane.

The MRI properties of serially diluted NanoQ were characterized in triplicate. By addition of ultrapure water, nine dilutions of the particles ranging from the concentration as prepared (i.e., 6.82×10^{-5} mM NanoQ) to 4.24×10^{-7} mM NanoQ were prepared. The nanoparticle concentration was estimated from the nominal particle size determined by laser light scattering and the total volume of polysorbate−Cu(II) incorporated into the NanoQ formulation. The dilutions were scanned at room temperature on clinical scanners with a transmit-and-receive birdcage head coil (Achieva, Philips Healthcare) to measure the R1 and R2 relation rates. A single-slice inversion recovery sequence (i.e., the Look−Locker technique)[8] was employed to calculate the ionic (per mM copper) and particulate (per mM NanoQ) r1 relaxivities at 1.5 and 3.0 T (resolution = 1 mm × 1 mm × 10 mm; 64 samples of the inversion recovery signal starting at 21 ms and spaced at 30 ms; sampling flip angle of 6°; TE = 1.62 ms; TR = 4 s; six averages). Similarly, the r2 relaxivity was measured using a multi-echo−spin-echo technique[9] (resolution = 1 mm × 1 mm × 10 mm; 15 echoes at 8 ms intervals; TR = 750 ms; two averages). The relaxivities (mean ± standard error) for the agent based on Cu concentrations were r1 = 4.26 ± 0.14 mM^{-1} s^{-1} and r2 = 8.7 ± 0.18 mM^{-1} s^{-1} at 1.5 T and r1 = 4.02 ± 0.19 mM^{-1} s^{-1} and r2 = 10.43 ± 0.34 mM^{-1} s^{-1} at 3 T. The ionic relaxivity values of NanoQ were comparable to those of commercially available Gd-based contrast agents (e.g., Magnevist, Gadovist, MultiHance).[10] The more relevant particulate relaxivities were r1 = 66 000 ± 2200 mM^{-1} s^{-1} and r2 = 135 000 ± 2900 mM^{-1} s^{-1} at 1.5 T and r1 = 62 000 ± 3000 mM^{-1} s^{-1} and r2 = 162 000 ± 5300 mM^{-1} s^{-1} at 3 T (Figure 2). The physical basis for the high particulate relaxivity of NanoQ is unproven but hypothesized to reflect the intercalation of cupric oleate within the hydrophobic aspect of the phospholipid surfactant, which potentially affords an adequate paramagnetic influence on the immediately surrounding water medium.

To demonstrate the concept and effectiveness of fibrin-bound NanoQ, acellular fibrin clots were formed on a suture in saline (see the SI) as a phantom target to which NanoQ was bound using a well-characterized and fibrin-specific (i.e., dog, human, pig) monoclonal antibody[11] and classic avidin−biotin chemistry.

dx.doi.org/10.1021/ja201918u | J. Am. Chem. Soc. 2011, 133, 9168–9171

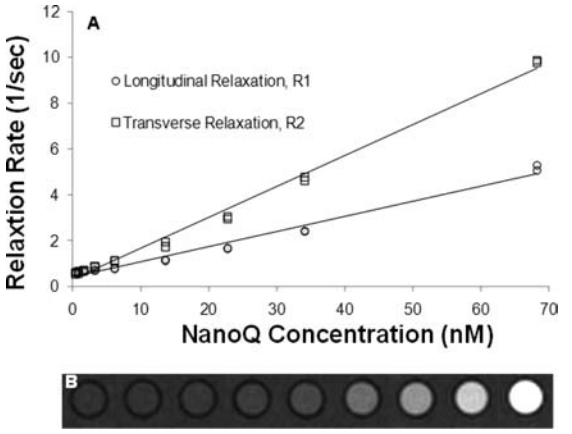

Figure 2. Relaxivity measurements of NanoQ. The relaxivities r_1 and r_2 were calculated from the measured relaxation rates as a function of contrast agent concentration. (A) Plots of replicate longitudinal relaxation rate (R1) and transverse relaxation rate (R2) data at 1.5 T. (B) Photograph showing T1-weighted MRI of the contrast agent diluted in water from (left to right) the lowest to the highest concentration tested.

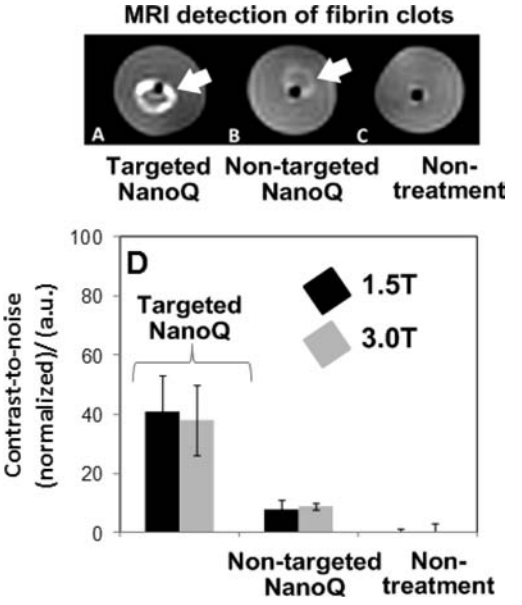

Figure 3. MRI detection of fibrin clots in vitro. (A–C) On T1-weighted cross-sectional images, the clot with targeted NanoQ (A) showed marked signal enhancement, whereas the controls of nontargeted contrast agent (B) and no treatment (C) showed little or no enhancement above the background water signal. (D) Normalized contrast-to-noise measurements of targeted and control NanoQ bound to clots with respect to the surrounding fluid.

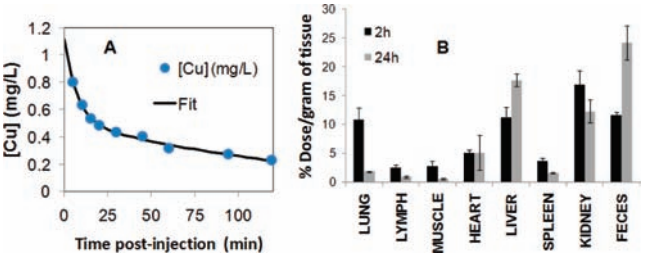

Figure 4. In vivo pharmacokinetics and biodistribution of NanoQ. (A) Pharmacokinetic profile of targeted NanoQ with a biexponential fit [$y = 0.5903\exp(-0.1374t) + 0.5205\exp(-0.0070t)$. (B) Organ distribution of NanoQ based on copper estimation of major organs by ICP–OES at 2 and 24 h following intravenous injection of NanoQ (1 mg/mL).

As controls, one clot was not treated and another was treated with nontargeted contrast agent. The clots in saline were imaged using T1-weighted techniques (TR = 25 ms; TE = 6.2 ms at 1.5 T and 3.9 ms at 3 T; flip angle = 30°; resolution = 0.5 mm × 0.5 mm × 1.0 mm) at 1.5 and 3.0 T. Strong T1w signal enhancement was appreciated along the periphery of the targeted phantom clot. The particles were excluded by size from penetrating into the dense fibrin weave of the acellular thrombus, consistent with previous studies using this experimental model. In contradistinction, the phantom clot was essentially unseen following exposure to the nontargeted agent or saline alone, confirming that the enhancement (corresponding to ~400% signal enhancement over the controls) was the result of the bound NanoQ alone (Figure 3). The quantitative MRI measurement [as signal intensity (SNR) normalized to the SNR of the surrounding fluid] of the fibrin clots targeted with NanoQ presented homogeneous T1w contrast enhancement with signal intensities of 1.41 ± 0.28, 1.08 ± 0.06 and 1.01 ± 0.03 au for targeted NanoQ, nontargeted NanoQ, and untreated clot, respectively, at 1.5 T. The results at 3 T were similar and resulted in T1w contrast enhancement with signal intensities of 1.38 ± 0.17, 1.09 ± 0.07, and 0.99 ± 0.09 au, respectively. The normalized signal intensity of the surrounding medium (nanopure water) was 1.00 ± 0.06 au at both 1.5 and 3 T.

The pharmacokinetics, biodistribution, and bioelimination of NanoQ were evaluated in rodents. Following intravenous administration, the concentration of copper in serial blood samples as a function of time was determined by ICP–OES (Figure 4A). In all animals ($n = 3$), a standard two-compartment biexponential model fit the data well ($R^2 > 0.99$). The closed-form solution to this model is the well-described expression $C(t) = Ae^{-\alpha t} + Be^{-\beta t}$, where the constants A and α describe the distribution phase and B and β the blood-clearance phase.[12] The half-lives (mean ± standard error) were 5.04 ± 1.1 and 99.2 ± 10.7 min for the distribution and elimination phases, respectively.

To define the in vivo biodistribution and acute safety profile in rats, copper-loaded NanoQ particles were injected intravenously at 1 mL (20 vol % emulsion)/kg of body weight. Tests for free hemoglobin in the urine with urine strips (Vetstrip; ARJ Medical) revealed no evidence of marked hemolysis. At 2 h after NanoQ injection, kidney and feces accumulated 16.9 ± 2.4 and 11.6 ± 0.5% injected dose (ID)/g of tissue, whereas lung and liver took up 10.9 ± 2.0 and 11.2 ± 1.8% ID/g of tissue. Spleen, heart, muscle and lymph accumulated smaller amounts of NanoQ as well (3.7 ± 0.5, 5.1 ± 0.5, 2.8 ± 0.9, and 2.5 ± 0.5% ID/g of tissue, respectively). Interestingly, some accumulation of NanoQ was noticed at 2 h in lung, which is typically not observed in similar systems. Further detailed investigation to study the in vivo biodistributive properties of these particles is warranted. At 24 h after NanoQ injection, feces, liver, and kidney were the sites of major accumulation (Figure 4B). Almost all other organs showed negligible copper content at that time. These data suggest that NanoQ presumably followed a typical biodistribution of particles into the reticuloendothelial system (RES) but that the copper organocomplexes were rapidly bioeliminated primarily through both the renal and biliary routes, as suggested by the metal

dx.doi.org/10.1021/ja201918u | J. Am. Chem. Soc. 2011, 133, 9168–9171

concentrations in the kidney and feces. Collectively, these data indicate that NanoQ has an optimal circulatory half-life for targeting intravascular thrombus. The particle is cleared from blood as expected through the normal RES organs, and the copper metal complexes are rapidly eliminated from the body.

In conclusion, we report an efficient, commercially amenable synthesis of a paramagnetic bivalent copper nanocolloid targeted to fibrin. The incorporation of copper as a metal complex allowed very high loading without resorting to the use of large, hard, solid metal particles, which greatly contributed to the desired pharmacokinetic, biodistribution, and bioelimination profiles in rats. The agent provided strong T1w contrast in vitro that exhibited nearly 3 times higher longitudinal relaxivity than previously reported gold−copper alloy nanoparticles. The high relaxivity and detection sensitivity of the copper nanocolloids are in the low nanomolar range, which point toward the potential utility of these agents for detection of microthrombi. NanoQ offers an effective, non-gadolinium-based T1w molecular imaging agent that could be applied to the diagnosis of ruptured unstable plaque in accessible vascular structures such as carotid arteries, which might be useful for delineating unstable lesions in acute vascular syndromes.

■ ASSOCIATED CONTENT

Supporting Information. Description of experimental methods and analytical measurements. This material is available free of charge via the Internet at http://pubs.acs.org.

■ AUTHOR INFORMATION

Corresponding Author
dipanjan@wustl.edu

■ ACKNOWLEDGMENT

The financial support from the AHA (0835426N), the NIH (Grants NS059302, CA119342, and HL073646), and the NCI (Grant N01CO37007) is greatly appreciated. We thank Mike J. Scott for his help with the clot experiment.

■ REFERENCES

(1) (a) Pasterkamp, G.; Falk, E. *J. Clin. Basic Cardiol.* **2000**, *3*, 81. (b) Fuster, V.; Badimon, L.; Badimon, J.; Chesebro, J. H. *N. Engl. J. Med.* **1992**, *326*, 242. 310. (c) Falk, E. *Am. J. Cardiol.* **1991**, *68* (Suppl. B), 28B. (d) Falk, E.; Shah, P. K.; Fuster, V. *Circulation* **1995**, *92*, 657. (e) Virmani, R.; Kolodgie, F. D.; Burke, A. P.; Farb, A.; Schwartz, S. M. *Arterioscler., Thromb., Vasc. Biol.* **2000**, *20*, 1262.

(2) (a) Waxman, S.; Ishibashi, F.; Muller, J. E. *Circulation* **2006**, *114*, 2390. (b) Maseri, A.; Fuster, V. *Circulation* **2003**, *107*, 2068. (c) Sharif, F.; Murphy, R. T. *Catheterization Cardiovasc. Interventions* **2010**, *75*, 135. (d) Briley-Saebo, K. C.; Mulder, W. J. M.; Mani, V.; Hyafil, F.; Amirbekian, V.; Aguinaldo, J. G. S.; Fisher, E. A.; Fayad, Z. A. *J. Magn. Reson. Imaging* **2007**, *26*, 460. (e) Phinikaridou, A.; Ruberg, F. L.; Hallock, K. J.; Qiao, Y.; Hua, N.; Viereck, J.; Hamilton, J. A. *Circ.: Cardiovasc. Imaging* **2010**, *3*, 323.

(3) (a) Winter, P. M.; Caruthers, S. D.; Wickline, S. A.; Lanza, G. M. *Nanofabrication Towards Biomedical Applications*; Wiley-VCH: Weinheim, Germany, 2005; pp 227−249 (b) Caruthers, S. D.; Wickline, S. A.; Lanza, G. M. *Curr. Opin. Biotechnol.* **2007**, *1*, 26. (c) Weissleder, R.; Kelly, K.; Sun, E. Y.; Shtatland, T.; Josephson, L. *Nat. Biotechnol.* **2005**, *23*, 1418. (d) Won, J.; Kim, M.; Yi, Y.-W.; Kim, Y. H.; Jung, N.; Kim, T. K. *Science* **2005**, *309*, 121.(e) Brown, M. A., Semelka, R. C. *MRI: Basic Principles and Applications*, 3rd ed.; Wiley-Liss: New York, 2003. (f) Artemov, D. J. *Cell. Biochem.* **2003**, *90*, 518. (g) Hawker, C. J.; Wooley, K. L. *Science* **2005**, *309*, 1200. (h) O'Reilly, R. K.; Hawker, C. J.; Wooley, K. L. *Chem. Soc. Rev.* **2006**, *35*, 1068. (i) Whitesides, G. M. *Small* **2005**, *1*, 172.(j) Hummel, H.; Weiler, V. U.; Hoffmann, R. PCT Int. Appl. WO2006064451A2, 2006. (k) Unger, E. C.; Fritz, T. A.; Gertz, E. W. U.S. Patent 6,139,819, Oct 31, 2000. (l) Nishiyama, N.; Kataoka, K. *Pharmacol. Ther.* **2006**, *11*, 630. (m) Wickline, S. A.; Lanza, G. M. J. *Cell. Biochem.* **2002**, *90* (Suppl. 39), 7. (n) Winter, P. M.; Morawski, A. M.; Caruthers, S. D.; Fuhrhop, R. W.; Zhang, H.; Williams, T. A.; Allen, J. S.; Robertson, J. D.; Lanza, G. M.; Wickline, S. A. *Circulation* **2003**, *108*, 2270. (o) Turner, J. L.; Pan, D.; Plummer, R.; Chen, Z.; Whittaker, A. K.; Wooley, K. L. *Adv. Funct. Mater.* **2005**, *15*, 1248.

(4) (a) Kuo, P. H. *J. Am. Coll. Radiol.* **2008**, *5*, 29. (b) Abu-Alfa, A. K. *J. Am. Coll. Radiol.* **2008**, *5*, 45. (c) Ersoy, H.; Rybicki, F. J. *J. Magn. Reson. Imaging* **2007**, *26*, 1190.

(5) (a) Senpan, A.; Caruthers, S. D.; Rhee, I.; Mauros, N. A.; Pan, D.; Hu, G.; Scott, M. J.; Fuhrhop, R. W.; Gaffney, P. J.; Wickline, S. A.; Lanza, G. M. *ACS Nano* **2009**, *3*, 3917. (b) Schellenberger, E. A.; Bogdanov, A., Jr.; Hogemann, D.; Tait, J.; Weissleder, R.; Josephson, L. *Mol. Imaging* **2002**, *1*, 102. (c) McAteer, M. A.; Sibson, N. R.; von Zur Muhlen, C.; Schneider, J. E.; Lowe, A. S.; Warrick, N.; Channon, K. M.; Anthony, D. C.; Choudhury, R. P. *Nat. Med.* **2007**, *13*, 1253. (d) Na, H. B.; Lee, J. H.; An, K.; Park, Y.; Park, M.; Lee, I. S.; Nam, D.-H.; Kim, S. T.; Kim, S.-H.; Kim, S.-W.; Lim, K.-H.; Kim, K.-S.; Kim, S.-O.; Hyeon, T. *Angew. Chem., Int. Ed.* **2007**, *46*, 5397. (e) Shin, J.; Anisur, R. M.; Ko, M. K.; Im, G. H.; Lee, J. H.; Lee, I. S. *Angew. Chem., Int. Ed.* **2009**, *48*, 321.

(6) (a) *Copper in Plant, Animal and Human Nutrition*; Copper Development Association (CDA) Publication TN35, 1988. (b) Benders, A. A.; Li, J.; Lock, R. A.; Bindels, R. J.; Bonga, S. E.; Veerkamp, J. H. *Pflugers Arch.* **1994**, *428*, 461.

(7) Su, C.-H.; Sheu, H.-S.; Lin, C.-Y.; Huang, C.-C.; Lo, Y.-W.; Pu, Y.-C.; Weng, J.-C.; Sheih, D.-B.; Chen, J.-H.; Yeh, C.-S. *J. Am. Chem. Soc.* **2007**, *129*, 2139.

(8) Look, D. C.; Locker, D. R. *Rev. Sci. Instrum.* **1970**, *41*, 621.

(9) Carr, H. Y.; Purcell, E. M. *Physiol. Rev.* **1954**, *94*, 630.

(10) Jorg, P.; Petros, M.; Hansjorg, G.; Kalus-Peter, L.; Claus, C.; Fritz, S. *Invest. Radiol.* **2006**, *41*, 213.

(11) Raut, S.; Gaffney, P. *J. Thromb. Haemostasis* **1996**, *76*, 56.

(12) Neubauer, A. M.; Sim, H.; Winter, P. M.; Caruthers, S. D.; Williams, T. A.; Robertson, J. D.; Sept, D.; Lanza, G. M.; Wickline, S. A. *Magn. Reson. Med.* **2008**, *60*, 1353.